

LUNAR REGOLITH DIELECTRIC CONSTANT INVERSION OF CHANG'E-1 MICROWAVE RADIOMETER RESULTS AT APOLLO 15. X. Gong^{1,2}, D. A. Paige², M. A. Seigler³, Y.Q. Jin¹, ¹Key Laboratory of Wave Scattering and Remote Sensing Information, Fudan University, Shanghai 200433, China (081021045@fudan.edu.cn), ²Department of Earth and Space Sciences, UCLA, ³Jet Propulsion Laboratory, California Institute of Technology, Pasadena, CA, USA.

Introduction: China's Chang'E-1(CE-1) microwave radiometer has measured the thermal emission from the moon at 3.0, 7.8, 19.35 and 37.0 GHz respectively [1]. The heat flow experiment on Apollo15 provided us with detailed information regarding the temperature variations at the surface and subsurface [2]. The infrared observations from the LRO Diviner Lunar Radiometer experiment [3] can also be used to validate surface temperatures at this site. We have combined the CE-1 microwave data at the Apollo 15 site with thermal model results at the Apollo 15 site [4] to derive best fit dielectric constants for the lunar regolith.

Methods: In 1984, Keihm [4] derived a set of thermophysical properties for lunar soil that match surface and subsurface temperature measurements from the Apollo 15 heat flow experiment. The soil bulk density is 1.25 g/cm³ for top 2 cm, and follows Equation 1 at depths greater than 2 cm.

$$\rho = 1.90 - 0.65 \exp((2 - z) / 4) \quad (z > 2\text{cm}) \quad (1)$$

Figures 1 and 2 show calculated surface and subsurface temperatures for the Keihm's model. Figure 1 also shows Diviner Channel 7 brightness temperatures ($\lambda=25\text{-}50\mu\text{m}$) for a 6×6 km box centered at the Apollo 15 landing site.

These temperature profiles were applied to calculate the microwave brightness temperatures. For nadir observations, the calculation method is shown in Equation (2)[5]:

$$T_B = [1 - r] \int_0^\infty \rho(x) \kappa_v(x) T(x) e^{-\int_0^x \rho(x') \kappa_v(x') dx'} dx \quad (2)$$

where $\kappa_v(x)$ is the mass extinction coefficient, $\rho(x)$ is the bulk density and r is the microwave reflectivity at the surface. For homogeneous medium, $\kappa_v(x)$ is a constant and internal reflections between layers is neglected. By comparing the simulation result from Eq.(2) with the microwave data from CE-1 at the same lunar local times, the best fit of r and κ_v for each channel can be found by using the least square's method. Based on these parameters, it is possible to calculate brightness temperatures over a whole diurnal cycle.

Results: A total of 75 observations at 7 different local times of CE-1 microwave data were collected within a $1^\circ \times 1^\circ$ box centered Apollo 15 landing site. Fig. 3 shows the CE-1 brightness temperatures in the

four channels and the best-fit calculated brightness temperatures as a function of local time.

Table 1 shows the best-fit model parameters and the derived dielectric constants for each channel. The frequency-normalized attenuation coefficient (κ_v/f) was found to be similar for all channels. The derived effective dielectric constant and specific loss tangent results are similar to those derived from ground-based observations [5].

Conclusions and Discussion: We have successfully fit the observed diurnal variations in the CE-1 microwave observations at the Apollo 15 site using a relatively simple thermal emission and absorption model based on independently-derived surface and subsurface temperatures. Our results show that the attenuation length-scale for the CE-1 microwave channels appears to be less than 1 meter, which suggests that CE-1 observations are sensitive primarily to near-surface regolith properties. Our best-fit microwave soil properties are strongly sensitive to the input temperature profiles, so the availability of ground-truth thermal data at the Apollo 15 landing site was critical for this study. We next plan to use subsurface temperatures derived from Diviner data and thermal models to produce global maps of CE-1 dielectric constants.

References: [1] J. Jiang, and Y.Q. Jin (2011) Selected Papers on Chinese Microwave Lunar Explorer Science Press. [2] M.G. Langseth, S. J. Keihm and K. Peters (1976) PLSC, 3143-3171 [3] D.A. Paige et al. (2009) SSR. [4] S. J. Keihm, (1984) Icarus, 60, 568-589 [5] D. L. Mitchell and I. D. Pater., (1994) Icarus, 110, 2-32

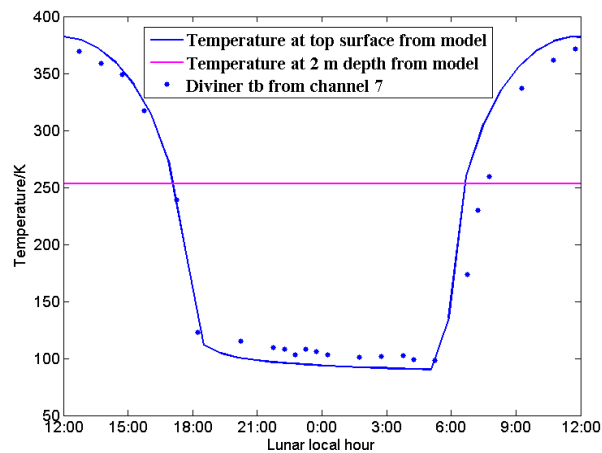


Fig.1 Diurnal temperature variations at the Apollo 15 site from Keihm (1984) [4] based on Apollo 15 heat flow measurements, and Diviner Channel 7 average measured brightness temperatures.

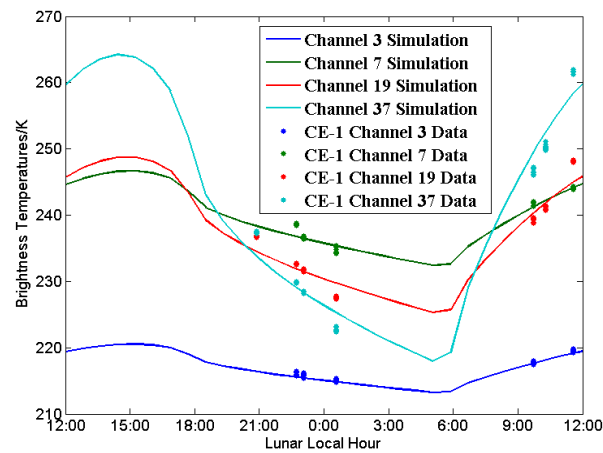


Fig. 3. Diurnal variations in Chang E-1 brightness temperatures the Apollo 15 landing site and best-fit model simulations.

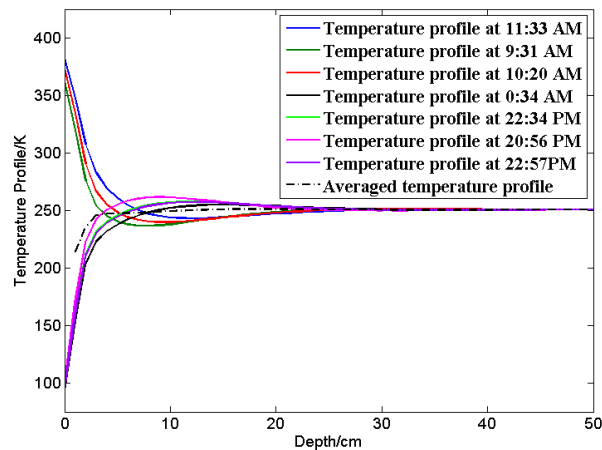


Fig.2. Temperature profiles as a function of depth at the Apollo 15 landing site from Keihm (1984) [4] based on Apollo 15 heat flow measurements.

Table1. Best fit CE-1 parameters at the Apollo 15 landing site.

Channel	λ (cm)	r	κ_v/f (m g/cm ³ Hz) ⁻¹	κ_v (m g/cm ³) ⁻¹	attenuation length (cm)	$\varepsilon(r)$	specific tan δ
37	0.8108	0.0300	1.2×10^{-10}	4.4400	11.85	2.012	0.0041
19	1.5504	0.0500	1.1×10^{-10}	2.1285	24.73	2.482	0.0034
7	3.8462	0.0425	1.6×10^{-10}	1.2480	42.17	2.307	0.0050
3	10.000	0.1345	2.3×10^{-10}	0.6900	76.28	4.656	0.0051